

## RESEARCH LETTER

10.1002/2016GL070302

## Key Points:

- A new drought index is developed based on estimated actual ET
- The new index equally performs with precipitation-dependent indices in areas of strong land-atmosphere coupling
- The new index spatially agrees with the Vegetation Health Index

## Correspondence to:

D. Kim,  
d.kim@apcc21.org

## Citation:

Kim, D., and J. Rhee (2016), A drought index based on actual evapotranspiration from the Bouchet hypothesis, *Geophys. Res. Lett.*, 43, 10,277–10,285, doi:10.1002/2016GL070302.

Received 8 JUL 2016

Accepted 27 SEP 2016

Accepted article online 28 SEP 2016

Published online 11 OCT 2016

## A drought index based on actual evapotranspiration from the Bouchet hypothesis

Dae-ha Kim<sup>1</sup> and Jinyoung Rhee<sup>1</sup>
<sup>1</sup>Climate Application Department, APEC Climate Center, Busan, South Korea

**Abstract** Global drought assessment has mainly depended on precipitation-based drought indices that may also take into account potential evapotranspiration ( $ET_p$ ). In this study, we combined the actual evapotranspiration ( $ET_a$ ) estimated from the Bouchet hypothesis and the structure of the Standardized Precipitation-Evapotranspiration Index to develop a fully ET-based drought index, the Standardized Evapotranspiration Deficit Index (SEDI). We found that SEDI, without using precipitation data, produces results that are consistent with the Palmer Drought Severity Index (PDSI) and the Standardized Precipitation Index (SPI) for drought identification in the South-Central United States. We also found a competitive performance of SEDI through comparisons between the Vegetation Health Index with SEDI, PDSI, and SPI. We suggest the high applicability of the SEDI based on the Bouchet hypothesis as an independent drought index for regions with strong land-atmosphere coupling or as an alternative drought index to fully precipitation-dependent indices for assessing agricultural droughts.

## 1. Introduction

Drought is a recurrent extreme climate event that may have detrimental consequences in human societies [Dai, 2011; Heim, 2002]. It is commonly characterized as the persistence of abnormally low precipitation, with general definitions including “a prolonged absence or marked deficiency of precipitation” [World Meteorological Organization, 1992] and “a period of abnormally dry weather sufficiently prolonged for the lack of precipitation to cause a serious hydrological imbalance” [American Meteorological Society, 1997]. From these definitions, the precipitation deficit is expected to play a central role in drought quantification and assessment. In several previous studies, the precipitation deficit was viewed as a main factor of increasing drought risk under climate change [e.g., Sheffield and Wood, 2008].

However, recent drought-related studies have focused mainly on evapotranspiration (ET) because it is coupled with atmospheric moisture demand and thus affects water availability on land surfaces [Dai, 2011]. Vicente-Serrano *et al.* [2010] proposed the Standardized Precipitation-Evapotranspiration Index (SPEI) by incorporating ET estimates into the structure of the Standardized Precipitation Index (SPI) [McKee *et al.*, 1993] and found more severe drought risks under global warming than are indicated by the precipitation deficit alone. Furthermore, a major controversy over global drought trends has originated from the discrepancy between the Thornthwaite and Penman-Monteith ET estimates [Sheffield *et al.*, 2012; Dai, 2013]. These studies suggest that ET could significantly affect drought severity, duration, and its spatial extent, and therefore, reliable ET estimates are essential for drought quantification.

Despite many attempts to include ET in drought assessment, most of previous studies have used ET with precipitation based on the concept of potential ET ( $ET_p$ ), which is a hypothetical measure of the evaporative demand. Importantly, they over-relied on proportionality between  $ET_p$  and actual ET ( $ET_a$ ), referred to as the Penman hypothesis [Han *et al.*, 2014], for estimating  $ET_a$ . Precipitation-based indices might be unsuitable for some practical purposes (e.g., drought forecasting) due to relatively higher uncertainty of precipitation than other climatic variables [Gao *et al.*, 2010]. In such a case, ET-based identification (i.e., comparison between  $ET_p$  and  $ET_a$ ) may be good to track drought conditions [e.g., Senay *et al.*, 2013]. With Penman hypothesis, however,  $ET_a$  cannot be determined without soil moisture information or a land surface model because water availability on land surfaces itself is required for obtaining  $ET_a$  [Allen *et al.*, 1998]. The use of precipitation data is hence ultimately inevitable for estimating  $ET_a$  when using the Penman hypothesis. Indeed, the Penman hypothesis is often rejected by decoupled relationships or negative correlations between  $ET_p$  and  $ET_a$  [e.g., Hobbins *et al.*, 2004; Ramirez *et al.*, 2005; Brutsaert, 2006]. The proportionality between  $ET_p$  and  $ET_a$  is still an open question on a controversy [Han *et al.*, 2014].

On the other hand, the complementary relationship (CR) methods [e.g., Morton, 1983; Granger and Gray, 1989] have practical advantages. It is based on the complementary feedback mechanism between the atmosphere and unsaturated land surfaces introduced by Bouchet [1963], suggesting an inverse relation between  $ET_p$  and  $ET_a$  (referred to as the Bouchet hypothesis hereafter). The Bouchet hypothesis is theoretically acceptable from the perspective of energy conservation and allows a reliable estimation of  $ET_a$  by solely using commonly available climatic data [Ma et al., 2015]. The CR methods have been advanced for several decades [e.g., Han et al., 2011; Anayah and Kaluarachchi, 2014] as an alternative for the standard methods based on the Penman hypothesis [e.g., Allen et al., 1998] but nevertheless has been barely used for drought characterization or assessment [Hobbins et al., 2016; McEvoy et al., 2016].

The main objective of this study is to develop a new drought index that is fully dependent on the variability of ET estimates using a recently proposed CR method. We investigated the applicability of the newly proposed index at 9 month time scale over the conterminous United States (CONUS) by comparing it with two conventional drought indices. We also evaluated performance of the new index for monitoring droughts in vegetative spheres using a remotely sensed drought index.

## 2. Methodology and Data

### 2.1. The Modified Granger and Gray Method

In the Bouchet hypothesis as illustrated in Figure 1, the wet-environment ET ( $ET_w$ ) is equal to  $ET_p$  and  $ET_a$  under saturated conditions, but the energy surplus increases  $ET_p$  as the surface dries (i.e.,  $ET_p > ET_w$ ). We used  $ET_w$  minus  $ET_a$  (referred to as ET deficit hereafter) to measure drought conditions because it should be closely related to surface water availability. Among the various CR methods used for estimating  $ET_w$  and  $ET_a$ , we selected the modified Granger and Gray (GG) method proposed by Anayah and Kaluarachchi [2014]. The modified GG method is a calibration-free method that was achieved through a comprehensive intercomparison study that considered modifications of the three classical CR methods of Morton [1983], Brutsaert and Stricker [1979], and Granger and Gray [1989]. It was validated by  $ET_a$  observations at 34 FLUXNET stations and showed statistically improved performance in  $ET_a$  estimation across a diverse range of climate conditions [see Anayah and Kaluarachchi, 2014].

The modified GG method uses the Priestley and Taylor equation [Priestley and Taylor, 1972] for estimating  $ET_w$  as

$$ET_w = \alpha \frac{\Delta}{\gamma + \Delta} (R_n - G_{soil}) \quad (1)$$

where  $\alpha$  is a coefficient with a value of 1.28,  $\Delta$  is the slope of the temperature-saturation vapor pressure curve ( $kPa^\circ C^{-1}$ ),  $\gamma$  is the psychrometric constant ( $kPa^\circ C^{-1}$ ), and  $R_n$  and  $G_{soil}$  are the net radiation ( $mm\ month^{-1}$ ) and the soil heat flux ( $mm\ month^{-1}$ ), respectively.  $R_n$  and  $G_{soil}$  are estimated with the maximum and minimum temperatures using the standard method of the American Society of Civil Engineers [Allen et al., 2005].

Granger and Gray [1989] developed an empirical relationship between  $ET_p$  and  $ET_a$  by defining the relative drying power ( $D$ ) and the relative ET ( $G$ ) as

$$D = \frac{E_a}{E_a + (R_n - G_{soil})} \quad (2a)$$

$$G = \frac{ET_a}{ET_p} = \frac{1}{1.0 + 0.028 \exp(8.045 D)} \quad (2b)$$

$$E_a = 10.6 \times (1 + 0.5U_2)(e_s - e_a) \quad (2c)$$

where  $E_a$  is the drying power of air ( $mm\ month^{-1}$ ),  $U_2$  is the wind speed at 2 m above the ground level, and  $e_s$  and  $e_a$  are the saturation and actual vapor pressures, respectively ( $mm\ Hg$ ).

The symmetric CR of Bouchet [1963] is used in the modified GG method as

$$ET_a = 2ET_w - ET_p \quad (3)$$

$ET_a$  is obtained from equations (2b) and (3) as

$$ET_a = \frac{2G}{G + 1} ET_w \quad (4)$$

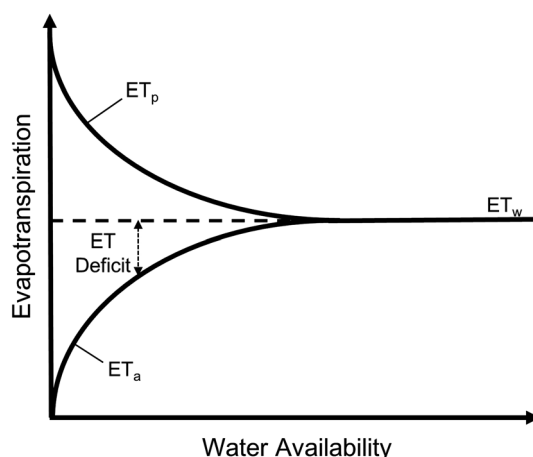


**Figure 1.** The complementary relationship between  $ET_p$  and  $ET_a$  and the ET deficit as drought indicator.

Further details and discussion about the modified GG method are available in Anayah and Kaluarachchi [2014].

## 2.2. Climatic Data and Drought Indices

We mainly used monthly gridded temperature data sets from the PRISM (Parameter-elevation Regressions on Independent Slopes Model) Climate Group (available at <http://www.prism.oregonstate.edu/>) that cover the CONUS at 4 km grid resolution from 1895 to 2014. The PRISM products are high-quality spatial climatic data acquired through a physiographical interpolation of point observa-

tions [Daly et al., 2008] and are regarded as enhanced climate data sets from knowledge-based mapping and a rigorous peer-review process [Kangas and Brown, 2007]. Detailed information about the PRISM data sets can be found at [http://www.prism.oregonstate.edu/documents/PRISM\\_datasets.pdf](http://www.prism.oregonstate.edu/documents/PRISM_datasets.pdf).

Due to the difficulty of collecting quality wind speed data with the same length of the PRISM data sets, we used normal values of gridded wind speed for the 12 months (i.e., 12 typical spatial variations of January through December were only considered). The normal values were obtained by averaging the gridded daily wind speed data at 4 km resolution from 1979 to 2014 provided by the University of Idaho Gridded Surface Meteorological Data (available at <http://climate.nkn.uidaho.edu/METDATA/>). We converted the wind speed at 10 m above the ground level using the power law for calculating  $E_a$ .

For relative humidity, we used estimates of dew point temperature ( $T_d$ ).  $T_d$  was estimated as the minimum temperature minus a temperature differential ranging from 0°C (for the lowest aridity) to 2.0°C (for the highest aridity) according to the recommendations for missing climatic data in Allen et al. [1998]. The aridity of each grid cell was identified by the ratio of annual precipitation to the Hargreaves ET, calculated using the 30 year normals of the PRISM data sets (available at <http://www.prism.oregonstate.edu/normal/>).

To evaluate drought indication of the new index, we additionally downloaded the Palmer Drought Severity Index (PDSI) and SPI data sets as per the official U.S. climate divisions from the National Climate Data Center (available at <http://www1.ncdc.noaa.gov/pub/data/cirs/drd/>). PDSI and SPI are highly or fully dependent on precipitation variability and have been commonly used for global and historical drought assessments [e.g., Dai, 2011]. We also collected the 4 km global Vegetation Health Index (VHI) products of advanced very high resolution radiometer from the Center for Satellite Applications and Research of the National Oceanic and Atmospheric Administration (available at [http://www.star.nesdis.noaa.gov/smcd/emb/vci/VH/vh\\_ftp.php](http://www.star.nesdis.noaa.gov/smcd/emb/vci/VH/vh_ftp.php)) to evaluate performance of the new index for indicating vegetation status. Global VHI products in the 30th week of each year (i.e., vegetation status in late July) from 1982 to 2014 were downloaded.

## 2.3. Drought Identification

We adopted the structure of SPEI [Vicente-Serrano et al., 2010] to produce a probability-based relative drought index. The precipitation minus the reference ET of SPEI was replaced with the ET deficit obtained from the modified GG method. Since SPI and SPEI show strong correlations with PDSI at 9 to 12 months of duration [e.g., Vicente-Serrano et al., 2010], we hypothesized that the 9 month duration for accumulating ET deficit would show high correlations with the precipitation-based indices. The accumulation of ET deficit considers influence of moisture availability in the previous months on the drought conditions of the current month. Hence, the series of 9 month ET deficit for each grid cell of the PRISM data sets over 119 years were fitted to a three-parameter log-logistic distribution (LL3) for each month using the probability-weighted moments [Hosking, 1990], as recommended by Beguería et al. [2014]. Using the fitted log-logistic distribution and the gridded 9 month ET deficit, monthly drought indices were produced from 1896 to 2014 at a 4 km grid

resolution. While the SPEI uses the nonexceedance probability ( $p$ ) of accumulated precipitation, the exceedance probability ( $1 - p$ ) of the 9 month ET deficit was standardized because the ET deficit inversely indicates water availability. The novel drought index derived from the ET deficit will be referred to as the Standardized Evapotranspiration Deficit Index (SEDI) hereafter.

The time series of 9 month SEDI (referred to as SEDI9 hereafter) at 4 km grid resolution was spatially aggregated into the divisions for consistency with the downloaded PDSI and 9 month SPI (referred to as SPI9 hereafter) data sets. The global VHI images given at 4 km resolution were also spatially averaged with boundaries of the climate divisions for comparison.

### 3. Results and Discussion

#### 3.1. Drought Identification by SEDI9

As shown in Figure 1, the ET deficit should be negatively related to surface moisture conditions and thus inversely expresses water availability (i.e., a larger value indicates less water availability). Because  $ET_a$  cannot exceed  $ET_w$  mathematically from equations (2b) and (4), the ET deficit is always positive as is precipitation. Hence, it would be possible to use a two-parameter probability density function, such as the gamma distribution, instead of LL3 when calculating the SEDI. It is noteworthy that the SEDI is an index that indirectly indicates moisture conditions on land surfaces with no involvement of precipitation.

Although several ET-based drought indices have been proposed using differences (or ratios) between  $ET_a$  and  $ET_p$  [e.g., Anderson *et al.*, 2011; Narasimhan and Srinivasan, 2005], they have required remotely sensed images or land surface models. SEDI is distinguishable from the existing ET-based indices because it only uses common operational meteorological data. SEDI enables to extend ET-based drought identification up to the length of monthly temperature data sets when using typical wind speed values and minimum temperatures for relative humidity. However, all ET-based drought indices, including SEDI, have uncertainty. This assessment of uncertainty is beyond the scope of the current study, which aims to introduce the applicability of the Bouchet hypothesis in identifying droughts. Future efforts should be directed at further assessment of the reliability of  $ET_a$  estimates since this would inherently improve ET-based drought indices.

Figure 2 shows that the spatial distributions of the drought areas defined by the SEDI9, PDSI, and SPI9 were consistent for several major droughts in the CONUS. The months in 1934 and 1956 were part of the Dust Bowl and Southwest droughts, respectively, which are often documented as the worst multiyear droughts in the twentieth century [Folger and Cody, 2014]. The drought areas defined by the SEDI9 in July 1934 were similar to the divisions in drought areas defined by the PDSI. The SEDI9 captured the serious drought conditions in Montana during the Dust Bowl drought, which recorded great economic losses [Cook *et al.*, 2007] as D2 or D3 areas, whereas the SPI9 did not. Interestingly, drought areas defined by the PDSI in the month of the Dust Bowl appeared to be an intermediate state between those of the SEDI9 and SPI9, which may be because the PDSI considers precipitation and  $ET_p$  together for drought quantification. The extreme drought centered in Texas and New Mexico in 1956 was captured by the SEDI9, albeit with less severity. Additionally, the SEDI9 clearly defined the severe droughts in the northern Great Plains that led to the widespread Yellowstone fire in 1988 as well as the critical drought experienced across Texas in 2011 [Folger and Cody, 2014].

Figure 3 shows the temporal correlations between the SEDI9 and the two conventional drought indices over the period of 1896–2014. The average of the temporal correlations over all climate divisions between the SEDI9 and PDSI was 0.52 (highest value was 0.72), and it was 0.51 between the SEDI9 and SPI9 (highest value was 0.78). Correlations between PDSI and SPI9 were very high with a range of 0.64–0.86 for all climate divisions as expected from the selected 9 month duration of SPI. From the correlation maps, it is indicated that consistency between ET deficit and precipitation deficiency is highest in the South-Central U.S. and decreases with increasing proximity to the Pacific or Atlantic Oceans. Importantly, the locations of high correlation to SPI9 ( $>0.6$ ) approximately coincide with the regions of strong interactions between soil moisture and precipitation, namely, “hot spots” of land-atmosphere coupling [Koster *et al.*, 2004, 2006]. Guo *et al.* [2006] found that the hot spots are likely to locate in the transition zones between arid and wet areas. The energy availability (not water availability) mainly controls  $ET_a$  in wet areas, while  $ET_a$  in arid areas is too small to entail significant effects on rainfall generation; thereby, the transition zones between humid and arid areas only can have  $ET_a$  sensitive to moisture conditions on land surfaces. The correlation maps in

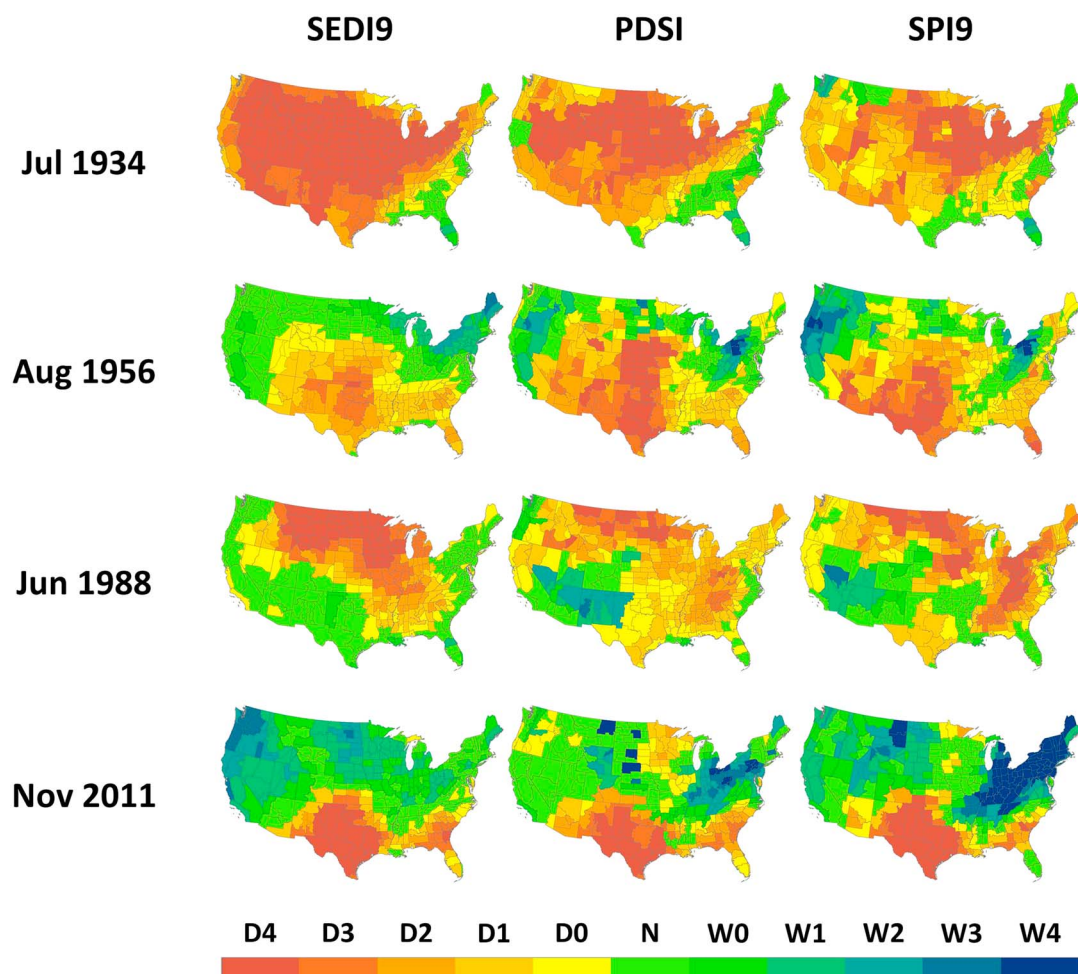


**Figure 2.** Maps of SEDI9, PDSI, and SPI9 for major drought months in the CONUS. The thresholds for classifying drought conditions (D4 to D0) were  $-2.0$ ,  $-1.6$ ,  $-1.3$ ,  $-0.8$ , and  $-0.5$  for the SEDI9 and SPI9, while those are  $-5.0$ ,  $-4.0$ ,  $-3.0$ ,  $-2.0$ , and  $-1.0$  for the PDSI. Wet conditions (W4 to W0) were categorized by the same numbers for D4 to D0 but with positive signs.  $N$  represents the normal condition.

Figure 3 confirm the hot spot locations of the prior studies [Koster *et al.*, 2004, 2006; Guo *et al.*, 2006] obtained from the atmospheric general circulation models. From the comparison between SEDI9, PDSI, and SPI9, we suggest that the combination of the modified GG method and the structure of SPEI can be a surrogate of precipitation-based drought indices in regions where the feedback mechanism between the atmosphere and land surfaces is expected to be strong.

Despite the ability for capturing drought conditions, the SEDI9 has caveats. First, it partially uses the CR since we defined droughts based on water availability (i.e.,  $ET_w - ET_a$ ), not on the evaporative demand (i.e.,  $ET_p$ ). For indicating drought conditions using the evaporative demand, the entire CR between  $ET_p$  and  $ET_a$  needs to be acknowledged [e.g., Hobbins *et al.*, 2016; McEvoy *et al.*, 2016]. It would be particularly important if an asymmetric CR is employed [e.g., Zuo *et al.*, 2016]. Second, temporal variation of wind speed needs to be considered because declining rates of wind speed are globally present [McVicar *et al.*, 2012]. We only considered spatial variation of wind speed for identifying the historical droughts in the early twentieth century, during which no quality wind speed data are available. However, impacts of the declining wind speed on the ET-based index should be further assessed since it gradually reduces the evaporative demand. In addition, the spatial scale should be appropriately selected for reliable estimation of  $ET_w$  and  $ET_a$  because the Bouchet hypothesis was developed under the assumption of negligible advection influences. At a very small or a continental scales, applying the same assumption could result in biased  $ET_a$  and  $ET_w$  estimates.



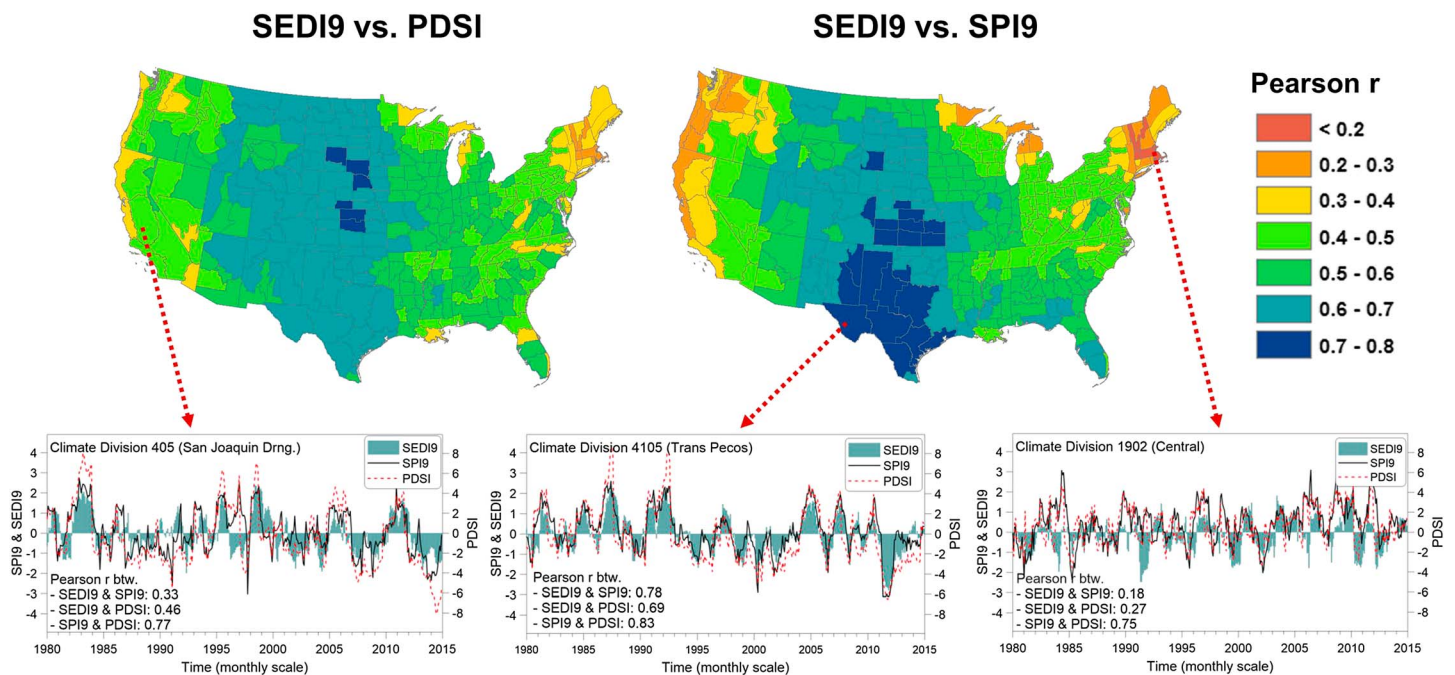


**Figure 3.** Distribution of temporal correlations (top left) between SEDI9 and PDSI and that (top right) between SEDI9 and SPI9 and (bottom) example time series of drought in three climate divisions.

### 3.2. Performance of SEDI for Vegetative Droughts

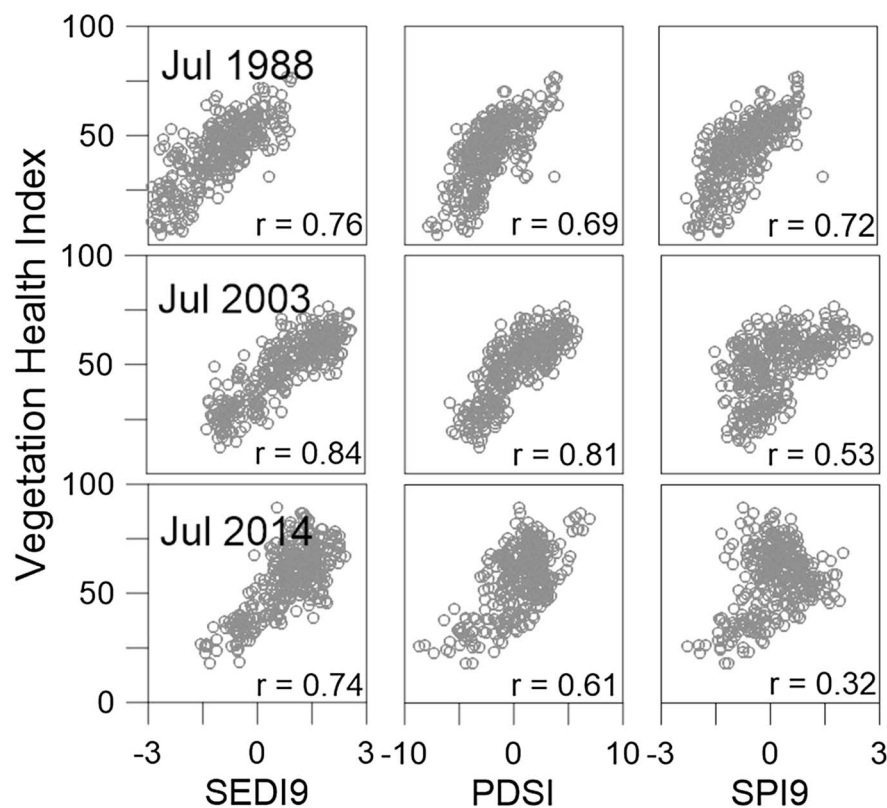
For evaluating performance of SEDI for indicating vegetative droughts, we compared VHI at the 30th week of the year (in the middle of growing season over the CONUS) with SEDI9, PDSI, and SPI9 in July from 1982 to 2014. VHI characterizes remotely sensed moisture and thermal conditions of vegetation surfaces. It is often used for assessing crop productivity, soil moisture conditions, and thus an indicator of agricultural droughts [Kogan *et al.*, 2004].

Figure 4 shows scatterplots between VHI and three indices of the climate divisions for the representative years with severe vegetative droughts [Kogan and Guo, 2015] and the time series of spatial correlations between VHI and the three drought indices. We found that SEDI9 was of clear positive correlations with VHI and generally outperforms SPI9 for indicating vegetative droughts. Average correlation coefficients for the period of 1982–2014 were 0.53, 0.60, and 0.41 between VHI and SEDI9, VHI and PDSI, and VHI and SPI9, respectively. Although PDSI was the best indicator of vegetation status on average, the performance of SEDI9 was comparable to PDSI. SEDI9 also performs better than the precipitation-dependent SPI9 in identifying agricultural droughts. In particular, the increasing trend in correlations between VHI and SEDI9 suggests that ET-based drought indices based on the Bouchet hypothesis could be better for monitoring agricultural and vegetative droughts in upcoming years. The upward correlation between VHI and SEDI9 may imply that the thermal condition is becoming relatively significant in indication of the vegetation health due to the globally rising temperatures.

## 4. Summary and Conclusions

A calibration-free method from the Bouchet hypothesis allowed us to estimate actual ET with readily available climatic data. A fully ET-dependent drought index was developed using the actual ET estimates in combination of the structure of a standardized drought index. The ET-based drought index was temporally consistent with conventional precipitation-based drought indices in identifying the historical droughts in the CONUS. High temporal correlations between the ET-based index and the precipitation-dependent indices were found in the regions with strong land-atmosphere coupling. From the comparison with the remotely sensed Vegetation Health Index, we also had an indication that the ET-based drought index well performs identifying vegetative or agricultural droughts.

a.



b.

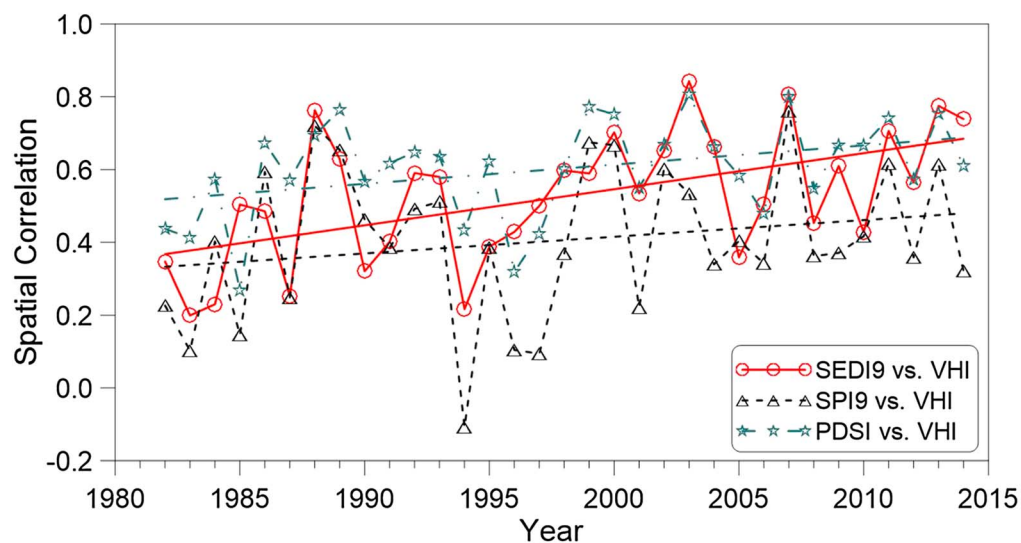


**Figure 4.** (a) Scatterplots between VHI and SEDI9, PDSI, and SPI9 for years with high correlation and (b) changes in spatial correlations between VHI and SEDI9, PDSI, and SPI9 over 1982–2014. The three straight lines inside the time series plots represent the linear trends of the spatial correlations.

ET has been central in recent scientific discussions on global and historical drought assessments, but most focus has been based on the application of the Penman hypothesis which depends on precipitation. The Bouchet hypothesis is an alternative approach for developing an ET-based index. In this study, we provided an example of a drought index based on the Bouchet hypothesis. Further studies could improve this work

and apply it to other related relevant topics. These may include drought identification in areas of weak land-atmosphere coupling, determining time scales of the ET-based index and its effects on drought definitions, impacts of globally declining wind speed, and linkage to other natural phenomena.

# Acknowledgments

The authors are grateful for the support of the APEC Climate Center for this study. The editing efforts of M. Bayani Cardenas and the constructive comments of anonymous reviewers are greatly appreciated. The drought index developed from this study and the data necessary to reproduce the results are available from the authors at request (d.kim@apcc21.org).

# References

- Allen, R. G., L. S. Pereira, D. Raes, and M. Smith (1998), Crop evapotranspiration: Guidelines for computing crop water requirement, FAO Irrig. Drain., Paper No. 56, Food and Agr. Orgn. of the United Nations, Rome.
- Allen, R. G., I. A. Walter, R. Elliot, T. Howell, D. Itenfisu, and M. Jensen (2005), The ASCE standardized reference evapotranspiration equation, environment and water resources Institute of the Am. Soc. Civil. Eng. (ASCE), Task Committee on Standardization of Reference Evapotranspiration, Final Rep., ASCE, Reston, Va.
- American Meteorological Society (1997), Meteorological drought—Policy statement, *Bull. Am. Meteorol. Soc.*, 78, 847–849.
- Anayah, F. M., and J. J. Kaluarachchi (2014), Improving the complementary methods to estimate evapotranspiration under diverse climatic and physical conditions, *Hydrol. Earth Syst. Sci.*, 18, 2049–2064, doi:10.5194/hess-18-2049-2014.
- Anderson, M. C., C. Hain, B. Wardlaw, A. Pimstein, J. R. Mecikalski, and W. P. Kustas (2011), Evaluation of drought indices based on thermal remote sensing of evapotranspiration over the conterminous United States, *J. Clim.*, 24, 2025–2044, doi:10.1175/2010JCLI3812.1.
- Beguería, S., S. M. Vicente-Serrano, F. Reig, and B. Latorre (2014), Standardized Precipitation Evapotranspiration Index (SPEI) revisited: Parameter fitting, evapotranspiration models, tools, datasets and drought monitoring, *Int. J. Climatol.*, 34, 3001–3023, doi:10.1002/joc.3887.
- Bouchet, R. J. (1963), Evapotranspiration réelle et potentielle, signification climatique, *Int. Assoc. Sci. Hydrol. Publ.*, 62, 134–142.
- Brutsaert, W. (2006), Indication of increasing land surface evaporation during the second half of the 20th century, *Geophys. Res. Lett.*, 33, L20403, doi:10.1029/2006GL027532.
- Brutsaert, W., and H. Stricker (1979), An advection aridity approach to estimate actual regional evaporation, *Water Resour. Res.*, 15, 443–450, doi:10.1029/WR015i002p00443.
- Cook, E. R., R. Seager, and M. A. Cane (2007), North American drought: Reconstructions, causes, and consequences, *Earth Sci. Rev.*, 81, 93–134, doi:10.1016/j.earscirev.2006.12.002.
- Dai, A. (2011), Characteristics and trends in various forms of the Palmer Drought Severity Index during 1900–2008, *J. Geophys. Res.*, 116, D12115, doi:10.1029/2010JD015541.
- Dai, A. (2013), Increasing drought under global warming in observations and models, *Nat. Clim. Change*, 3, 52–58, doi:10.1038/nclimate1633.
- Daly, C., M. Halbleib, J. I. Smith, W. P. Gibson, M. K. Doggett, G. H. Taylor, J. Curtis, and P. P. Pasteris (2008), Physiographically sensitive mapping of climatological temperature and precipitation across the conterminous United States, *Int. J. Climatol.*, 28, 2031–2064, doi:10.1002/joc.1688.
- Folger, P., and B. A. Cody (2014), Drought in the United States: Causes and current understanding, Congressional Research Service, Report 7–5700, R43407. [Available at <http://www.crs.gov>.]
- Gao, H., Q. Tang, C. R. Ferguson, E. F. Wood, and D. P. Lettenmaier (2010), Estimating the water budget of major U.S. river basins via remote sensing, *Int. J. Remote Sens.*, 31, 3955–3978.
- Granger, R. J., and D. M. Gray (1989), Evaporation from natural unsaturated surfaces, *J. Hydrol.*, 111, 21–29, doi:10.1016/00221694(89)90249-7.
- Guo, Z., et al. (2006), GLACE: The Global Land–Atmosphere Coupling Experiment. Part II: Analysis, *J. Hydrometeorol.*, 7, 611–625, doi:10.1175/jhm511.1.
- Han, S., H. Hu, D. Yang, and F. Tian (2011), A complementary relationship evaporation model referring to the Granger model and the advection-aridity model, *Hydrol. Process.*, 25, 2094–2101, doi:10.1002/hyp.7960.
- Han, S., F. Tian, and H. Hu (2014), Positive or negative correlation between actual and potential evaporation? Evaluating using a nonlinear complementary relationship model, *Water Resour. Res.*, 50, 1322–1336, doi:10.1002/2013WR014151.
- Heim, R. R., Jr. (2002), A review of twentieth-century drought indices used in the United States, *Bull. Am. Meteorol. Soc.*, 83, 1149–1165.
- Hobbins, M. T., J. A. Ramirez, and T. C. Brown (2004), Trends in pan evaporation and actual evapotranspiration across the conterminous U.S.: Paradoxical or complementary?, *Geophys. Res. Lett.*, 31, L13503, doi:10.1029/2004gl0198426.
- Hobbins, M. T., A. Wood, D. J. McEvoy, J. L. Huntington, C. Morton, M. Anderson, and C. Hain (2016), The Evaporative Demand Drought Index: Part I—Linking drought evolution to variations in evaporative demand, *J. Hydrometeorol.*, 17, 1745–1761, doi:10.1175/jhm-d-15-0121.1.
- Hosking, J. R. M. (1990), L-moments: Analysis and estimation of distributions using linear combinations of order statistics, *J. R. Stat. Soc. Ser. B*, 52, 105–124.
- Kangas, R. S., and T. J. Brown (2007), Characteristics of US drought and pluvials from a high-resolution spatial dataset, *Int. J. Climatol.*, 27, 1303–1325, doi:10.1002/joc.1473.
- Kogan, F., and W. Guo (2015), 2006–2015 mega-drought in the western USA and its monitoring from space data, *Geomatic Nat. Hazard Risk*, 6, 651–668, doi:10.1080/19475705.2012.1079265.
- Kogan, F., R. Stark, A. Gitelson, L. Jargalsaikhan, C. Dugrajav, and S. Tsooj (2004), Derivation of pasture biomass in Mongolia from AVHRR-based Vegetation Health Index, *Int. J. Remote Sens.*, 25, 2889–2896.
- Koster, R. D., et al. (2004), Regions of strong coupling between soil moisture and precipitation, *Science*, 305, 1138–1140, doi:10.1126/science.1100217.
- Koster, R. D., et al. (2006), GLACE: The Global Land–Atmosphere Coupling Experiment. Part I: Overview, *J. Hydrometeorol.*, 7, 590–610, doi:10.1175/jhm510.1.
- Ma, N., Y. Zhang, J. Szilagyi, Y. Guo, J. Zhai, and H. Gao (2015), Evaluating the complementary relationship of evapotranspiration in the alpine steppe of the Tibetan Plateau, *Water Resour. Res.*, 51, 1069–1083, doi:10.1002/2014WR015493.
- McEvoy, D. J., J. L. Huntington, M. T. Hobbins, A. Wood, C. Morton, M. Anderson, and C. Hain (2016), The Evaporative Demand Drought Index. Part II: CONUS-wide assessment against common drought indicators, *J. Hydrometeorol.*, 17, 1763–1779, doi:10.1175/jhm-d-15-0122.1.
- McKee, T. B. N., J. Doesken, and J. Kleist (1993), The relationship of drought frequency and duration to time scales, in *Proceedings of Eighth Conference on Applied Climatology*, pp. 179–184, Am. Meteorol. Soc., Anaheim, Calif.
- McVicar, T. R., et al. (2012), Global review and synthesis of trends in observed terrestrial near-surface wind speeds: Implications for evaporation, *J. Hydrol.*, 416–417, 182–205, doi:10.1016/j.jhydrol.2011.10.024.
- Morton, F. I. (1983), Operational estimates of areal evapotranspiration and their significance to the science and practice of hydrology, *J. Hydrol.*, 66, 1–76, doi:10.1016/j.jrse.2007.04.015.



- Narasimhan, B., and R. Srinivasan (2005), Development and evaluation of Soil Moisture Deficit Index (SMDI) and Evapotranspiration Deficit Index (ETDI) for agricultural drought monitoring, *Agric. For. Meteorol.*, *133*, 69–88, doi:10.1016/j.agrformet.2005.07.012.
- Priestley, C. H., and R. J. Taylor (1972), On the assessment of surface heat flux and evaporation using large-scale parameters, *Mon. Weather Rev.*, *100*, 81–92, doi:10.1175/15200493(1972)100<0081:OTAOSH>2.3.CO;2.
- Ramírez, J. A., M. T. Hobbins, and T. C. Brown (2005), Observational evidence of the complementary relationship in regional evaporation lends strong support for Bouchet's hypothesis, *Geophys. Res. Lett.*, *32*, L15401, doi:10.1029/2005GL023549.
- Senay, G. B., S. Bohms, R. K. Singh, P. H. Gowda, N. M. Velpuri, H. Alemu, and J. P. Verdin (2013), Operational evapotranspiration mapping using remote sensing and weather datasets: A new parameterization for the SSEB approach, *J. Am. Water Resour. Assoc.*, *49*, 577–591, doi:10.1111/jawr.12057.
- Sheffield, J., and E. F. Wood (2008), Projected changes in drought occurrence under future global warming from multi-model, multi-scenario, IPCC AR4 simulations, *Clim. Dyn.*, *31*, 79–105, doi:10.1007/s00382-007-0340-z.
- Sheffield, J., E. F. Wood, and M. L. Roderick (2012), Little change in global drought over the past 60 years, *Nature*, *491*, 435–438, doi:10.1038/nature11575.
- Vicente-Serrano, S. M., S. Beguería, and J. I. López-Moreno (2010), A multiscalar drought index sensitive to global warming: The Standardized Precipitation Evapotranspiration Index (SPEI), *J. Clim.*, *23*, 1696–1718.
- World Meteorological Organization (1992), *International Meteorological Vocabulary*, WMO No.182, 2nd ed., pp. 784, WMO.
- Zuo, H., B. Chen, S. Wang, Y. Guo, B. Zuo, L. Wu, and X. Gao (2016), Observational study on complementary relationship between pan evaporation and actual evapotranspiration and its variation with pan type, *Agric. For. Meteorol.*, *222*, 1–9, doi:10.1016/j.agrformet.2016.03.002.